University of Plymouth

PEARL **https://pearl.plymouth.ac.uk**

Faculty of Science and Engineering School of Engineering, Computing and Mathematics

2015-08

The effects of unequal compressive/tensile moduli of composites

Meng, M

http://hdl.handle.net/10026.1/3442

10.1016/j.compstruct.2015.02.064
Composite Structures

All content in PEARL is protected by copyright law. Author manuscripts are made available in accordance with publisher policies. Please cite only the published version using the details provided on the item record or document. In the absence of an open licence (e.g. Creative Commons), permissions for further reuse of content should be sought from the publisher or author.

Accepted Manuscript

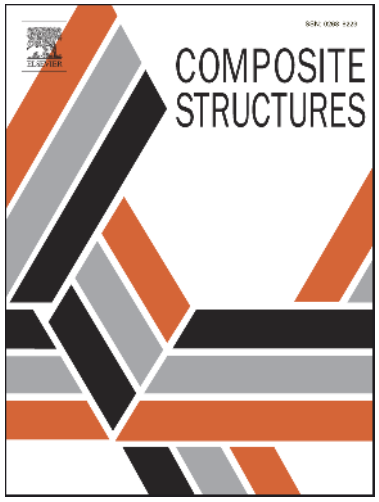

The effects of unequal compressive/tensile moduli of composites

M. Meng, H.R. Le, M.J. Rizvi, S.M. Grove

PII: S0263-8223(15)00152-X
DOI: http://dx.doi.org/10.1016/j.compstruct.2015.02.064
Reference: COST 6249

To appear in: *Composite Structures*

Please cite this article as: Meng, M., Le, H.R., Rizvi, M.J., Grove, S.M., The effects of unequal compressive/tensile moduli of composites, *Composite Structures* (2015), doi: http://dx.doi.org/10.1016/j.compstruct.2015.02.064

This is a PDF file of an unedited manuscript that has been accepted for publication. As a service to our customers we are providing this early version of the manuscript. The manuscript will undergo copyediting, typesetting, and review of the resulting proof before it is published in its final form. Please note that during the production process errors may be discovered which could affect the content, and all legal disclaimers that apply to the journal pertain.

ACCEPTED MANUSCRIPT

The effects of unequal compressive/tensile moduli of composites

M. Meng*, H. R. Le, M. J. Rizvi, S. M. Grove

School of Marine Science and Engineering, Plymouth University, United Kingdom

*Fax: +44 (0)1752 586101; email address: maozhou.meng@plymouth.ac.uk

Abstract

This paper investigates the effects of unequal compressive and tensile moduli of carbon fibre reinforced plastic (CFRP) composites. The basic assumption is based on the statistics that the compressive modulus is a fraction lower than the tensile modulus. Data evaluated by Finite Element Analysis (FEA) model, Classical Laminate Theory (CLT) model, and experiment are used to investigate these effects. The terms of compressive modulus are successfully introduced into the Tsai-Wu failure criterion for the production of failure envelops, into the Classical Beam Theory (CBT) and CLT for the investigation of flexural behaviour as well as the fibre microbuckling model for the analysis of compressive failure. The study shows that the failure criteria shift from stress domain to strain domain when the compressive modulus is considered, and the strain dominated failure criteria could generally provide more accurate prediction in composite material. Therefore it is proposed to apply strain dominated failure criteria for composite design, testing and certificate.

Keywords: Compressive modulus, Failure criterion, Classical Laminate Theory (CLT), Finite element analysis (FEA), Microbuckling

ACCEPTED MANUSCRIPT

ACCEPTED MANUSCRIPT

1. Introduction

The use of high strength, lightweight carbon fibre reinforced plastic (CFRP) composites in renewable energy devices is growing steadily due to their superior anti-corrosion properties and the long-term fatigue performance [1, 2]. According to the UK Engineering Integrity Society[3], a record of 22% of the UK's electricity supply was generated by wind. In other EU countries such as Germany, Spain and Denmark the record is approximately double. For many commercial CFRP composites, the longitudinal tensile strength can be five times higher than stainless streel with only one-fifth of its density. Besides the benefit of weight savings, it is possible to construct a rather huge structure for the renewable energy devices, such as the next-generation turbine blade.

In practical composite structures, the composite materials are subjected to complicated loading conditions, such as bending, tension, compression and twisting. A recent report of 3D FEA analysis[4] has demonstrated that all of the six stress components (σ_i, τ_{ij}) contribute to the failure criterion of CFRP composites, particularly the initiation of failure in bending. However, most of the previous studies on composites are based on equal compressive/tensile moduli, which may lead to either overestimate or underestimate the composite strength. The effects of unequal compressive/tensile moduli on the failure criterion of composites have not been reported.

Due to the fibre misalignment and manufacturing defects, the compressive modulus of long fibre composites is reasonably not expected to be equal to the tensile modulus [5-9]. This becomes important in flexural behaviour because the composites are under both compression and tension. A laminate with unequal moduli may not behave symmetrically in bending, such as the stress and strain distributions through-thickness, even though the layup is symmetric. Therefore, for many classical theories, such as Classical Beam Theory (CBT) and Classical Laminate Theory (CLT), the compressive modulus should be introduced in order to eliminate the unequal terms.

Several papers have described work to modify CBT in the flexural test for fibre reinforced plastic composites. Chamis [10-12] used continuum mechanics to derive the formula of maximum deflection in three-point bending using unequal compressive and tensile moduli. Zhou and Davies [13, 14] used statistical methods and assumed a higher compressive modulus to characterize the failure mechanics of thick glass woven roving/polyester laminates. Mujika et al. [15, 16] used strain gauges to determine the compressive and tensile moduli of unidirectional laminates by measuring the compressive strain and tensile strain at the top and bottom surfaces of specimens in three-point and four-point bending. However, the effects of unequal moduli on the flexural properties and the failure strength of multi-directional filament laminate composites have not been well understood.

In the present work, the compressive modulus is assumed to be a fraction lower than the tensile modulus based on the statistics of current commercial CFRP composites. The effects of unequal compressive/tensile moduli on composites are investigated: (a) the composite failure criterion, particularly Tsai-Wu failure criterion, (b) a modified CBT for the flexural properties of unidirectional laminate and its failure mechanisms, (c) a modified CLT for the

ACCEPTED MANUSCRIPT

flexural properties of multi-directional laminate, and (d) fibre micro-buckling. Three research approaches are used in parallel: (a) Finite Element Analysis (FEA) is employed to investigate the stress and strain distributions within the laminates for the identification of the maximum critical strains and stresses, (b) CLT is applied to extract the flexural modulus and strain/stress distributions of multi-directional laminate with different stacks, and (c) experiment is carried out to provide the sufficient evidence to support this study.

2. Background

Considering the loading condition and possible micro-scale structural defects in long fibre reinforced plastics composites, the compressive modulus is likely to be different from the tensile modulus. This will be more obvious in CFRP than GFRP composites since the diameter of carbon fibre is normally smaller than that of glass fibre. It is well-known that the smaller diameter of carbon fibre performs higher tensile strength. However, according to the Euler beam theory, a beam with smaller cross-section also tends to be unstable (buckling) which may lead to lower compressive strength. This is the dilemma in composite manufacturing.

Table 1. Longitudinal tensile/compressive moduli of CFRP composites and their strengths

	E_1^t (GPa)	E_1^c (GPa)	$\frac{E_1^c}{E_1^t}$	$(\sigma_1^t)_{ult}$ (GPa)	$(\sigma_1^c)_{ult}$ (GPa)	$\frac{(\sigma_1^c)_{ult}}{(\sigma_1^t)_{ult}}$
Celion 12k/938	136	119	0.87	1.88	1.39	0.74
AS4 12k/3502	133	124	0.93	1.78	1.41	0.79
HITEX 33 6k/E7K8	125	118	0.94	2.16	1.44	0.67
AS4 12k/938	154	125	0.81	2.17	1.57	0.73
AS4/3501-6	135	123	0.91	2.01	1.45	0.72
T300 15k/976	135	129	0.95	1.45	1.30	0.89
AS4 12k/997	137	123	0.89	2.25	1.58	0.70
IM6 12k/APC-2	149	134	0.90	2.41	1.15	0.48
HTS40/977-2[17]	140	112	0.80	2.52	1.40	0.56
Cytec/977-2 [18]	165	152	0.92	2.69	1.59	0.59
Avg.	141	126	0.89	2.13	1.43	0.69
SDs	12	11	0.05	0.37	0.14	0.12
Coeff var	8.4%	8.7%	5.8%	17.3%	9.5%	17.5%

*Data source: Polymer matrix composites material handbook [19]. The values were measured at 75°F (23°C), and normalized to $V_f = 60\%$

In Table 1, there are ten commercial CFRP composites and their ratios of compressive/tensile moduli are very close. For these CFRP composites, the average ratio of compressive modulus to tensile modulus is around 0.9. In fact, with the increase of statistical specimens, the standard deviation decreases and the coefficient of variation has a tiny drop from 5.8% to 4.6%, as shown in Fig. 1. The actual value depends on the volume fraction of fibres and the manufacturing process. The ratios of compressive/tensile strengths are also included in the statistics, and the average value presents around 60%-70%.

ACCEPTED MANUSCRIPT

For the convenient expression, a parameter is introduced to indicate the ratio of longitudinal compressive modulus to tensile modulus,

$$\lambda = \frac{E_1^c}{E_1^t} \tag{1}$$

Fig. 1 shows the λ value of various commercial CFRP and GFRP composites, and their coefficient of variation. The fibre volume fraction of CFRP and GFRP composites were normalized to $V_f = 60\%$ and $V_f = 50\%$ respectively. For a typical FRP composite, the diameters of carbon fibre and glass fibre are 7 μm and 25 μm respectively; therefore, the GFRP composites present relative higher λ value.

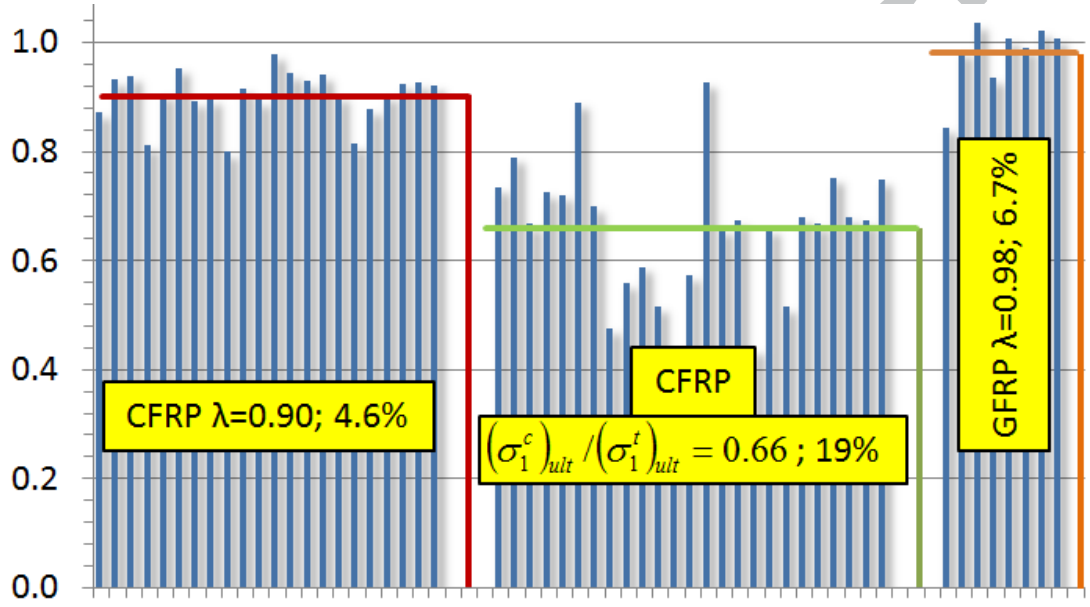

Fig. 1. Ratio of longitudinal compressive modulus to tensile modulus of various CFRP and GFRP. The average and their respective coefficient of variation are also shown in the figure.

There are two possible reasons of lower compressive modulus and compressive strength in CFRP which are inevitable in the manufacturing process: the fibre misalignment and void content. Employing the microscope image of the cross-section of unidirectional laminate, it is possible to do the statistics of fibre misalignment. Fig. 2 gives an indirect approach to measure the misalignment angle in a long fibre laminate. If it is assumed that the fibre is perfectly circular, the project of the fibre cross-section on horizontal plane is an ellipse, and the misalignment angle could be calculated by the ratio of short/long radius,

$$\theta_1 = \sin^{-1}(r_2 / r_1) \tag{2}$$

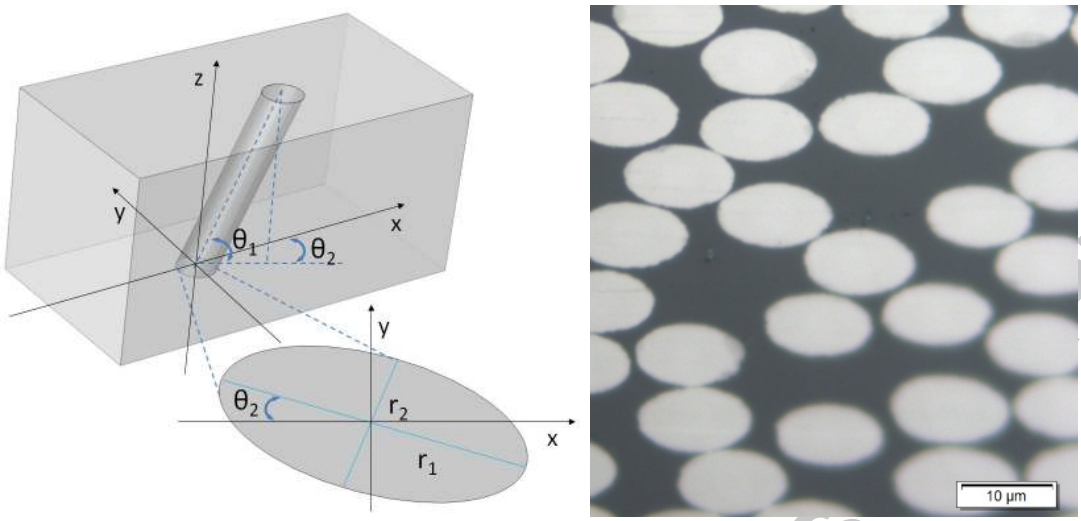

Fig. 2. Schematics of the measurement of fibre misalignment in a long fibre UD laminate (left), and a typical microscope image of the cross-section of UD laminate (right)

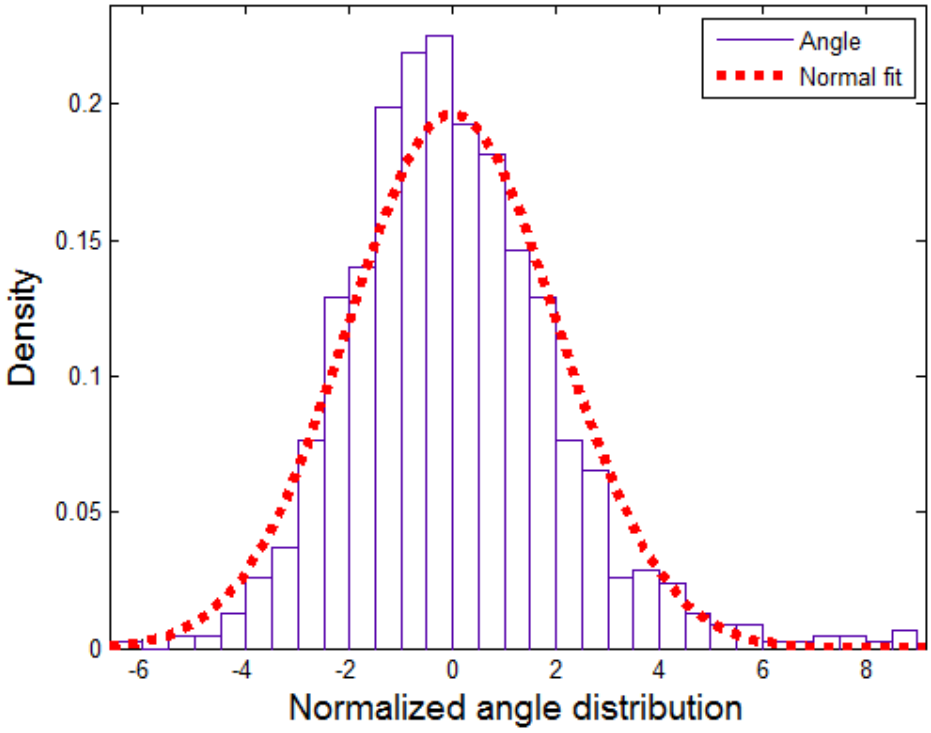

Fig. 3. Normalized fibre misalignment in long fibre CFRP composite. Approximate ten thousand specimens are included in the statistics.

Fig. 3 shows the normalized angle of fibre misalignment of HTS-12K/977-2 unidirectional laminate ($V_f = 57.9\%$). The laminate was hand-layup and autoclave-cured at a vacuum bag with a step of 3°C/min elevated temperature, and was dwelled at 180°C for two hours following cool-down at room temperature. The distribution of misalignment angles show a good fit to normal distribution (Gaussian distribution),

ACCEPTED MANUSCRIPT

$$f(\theta_1) = \frac{1}{\sqrt{2\pi}\sigma_0} \exp\left(-\frac{(\theta_1 - \mu_0)^2}{2\sigma_0^2} \right) \tag{3}$$

where μ_0 and σ_0 are the parameter of expectation and standard deviation respectively. For HTS-12K/977-2 unidirectional laminate $\mu_0 = 0, \sigma_0 = 2.03$.

In Fig. 3, it can be seen that the misalignment angle can extend up to ±6°. Although the spectral density of these angles is very small, the compressive failure may well initialize from these fibres and propagate through the whole laminate, and as a consequence the compressive strength is expected lower than tensile strength.

3. Failure criterion

It has been shown that unequal compressive/tensile moduli of the CFRP composites commonly exist and the average λ value is 0.9 with very small coefficient of variation. It means that the ultimate compressive strain of CFRP composites is underestimated by traditional failure criteria. Therefore, strain dominated failure criteria could more generally reflects the real conditions, and the failure envelop should be presented in strain space rather than stress space.

Tsai-Wu failure criterion [20], which includes compressive terms, is used in the present work to illustrate the effects of unequal compressive/tensile moduli of CFRP composites,

$$F_{ij}\sigma_i\sigma_j + F_i\sigma_i = 1 \tag{4}$$

$$\begin{aligned} F_{11} &= \frac{1}{\left(\sigma_1^t\right)_{ult}\left(\sigma_1^c\right)_{ult}}, F_1 = \frac{1}{\left(\sigma_1^c\right)_{ult}} - \frac{1}{\left(\sigma_1^t\right)_{ult}} \\ F_{22} &= \frac{1}{\left(\sigma_2^t\right)_{ult}\left(\sigma_2^c\right)_{ult}}, F_1 = \frac{1}{\left(\sigma_2^c\right)_{ult}} - \frac{1}{\left(\sigma_2^t\right)_{ult}} \\ F_{12} &= -0.5, F_{66} = \left(\frac{1}{\tau_{12}^{ult}}\right)^2 \end{aligned} \tag{5}$$

The criterion is quadratic and is expressed in stress space. In fact, most of the current failure criteria are expressed in stress space. Tsai-Wu failure criterion can be transformed to strain space by applying the relationship of extensional stiffness matrix [20],

$$U_{ij}\varepsilon_i\varepsilon_j + U_i\varepsilon_i = 1 \tag{6}$$

$$\begin{aligned} U_{ij} &= F_{kl}Q_{ki}Q_{lj} \\ U_i &= F_jQ_{ij} \end{aligned} \tag{7}$$

$$Q_{11}=\frac{E_1}{1-\nu_{12}\nu_{21}},Q_{22}=\frac{E_2}{1-\nu_{12}\nu_{21}}$$
$$Q_{12}=Q_{21}=\frac{\nu_{12}E_2}{1-\nu_{12}\nu_{21}},Q_{66}=G_{12} \quad (8)$$

Tsai-Wu failure criterion is fully defined in strain space by equations (4-8). According to Tsai's invariant-based theory[21], a transformation can be applied on the strain envelop to define the rotated strain envelops of all ply orientations,

$$\begin{bmatrix}\overline{U_{11}}\\ \overline{U_{22}}\\ \overline{U_{12}}\\ \overline{U_{66}}\\ \overline{U_{16}}\\ \overline{U_{26}}\\ \overline{U_1}\\ \overline{U_2}\\ \overline{U_6}\end{bmatrix}=\begin{bmatrix}1&0&0&0&0&0\\0&1&0&0&0&0\\0&0&1&0&0&0\\0&0&0&1&0&0\\\frac{3}{8}&-\frac{1}{8}&-\frac{1}{4}&-\frac{1}{2}&0&0\\\frac{1}{8}&-\frac{3}{8}&\frac{1}{4}&\frac{1}{2}&0&0\\0&0&0&0&1&0\\0&0&0&0&0&1\\0&0&0&0&\frac{1}{2}&-\frac{1}{2}\end{bmatrix}\begin{bmatrix}U_{11}\\U_{22}\\U_{12}\\U_{33}\\U_1\\U_2\end{bmatrix}\begin{bmatrix}1\\\cos 2\theta\\\cos 4\theta\\\sin 2\theta\\\sin 4\theta\\1\\\cos 2\theta\\\sin 2\theta\end{bmatrix} \quad (9)$$

$$\overline{U_{11}}\varepsilon_1^2+\overline{U_{22}}\varepsilon_2^2+2\overline{U_{12}}\varepsilon_1\varepsilon_2+2\overline{U_{16}}\varepsilon_1\varepsilon_6+$$
$$2\overline{U_{26}}\varepsilon_2\varepsilon_6+\overline{U_{66}}\varepsilon_6^2+\overline{U_1}\varepsilon_1+\overline{U_2}\varepsilon_2+\overline{U_6}\varepsilon_6=1 \quad (10)$$

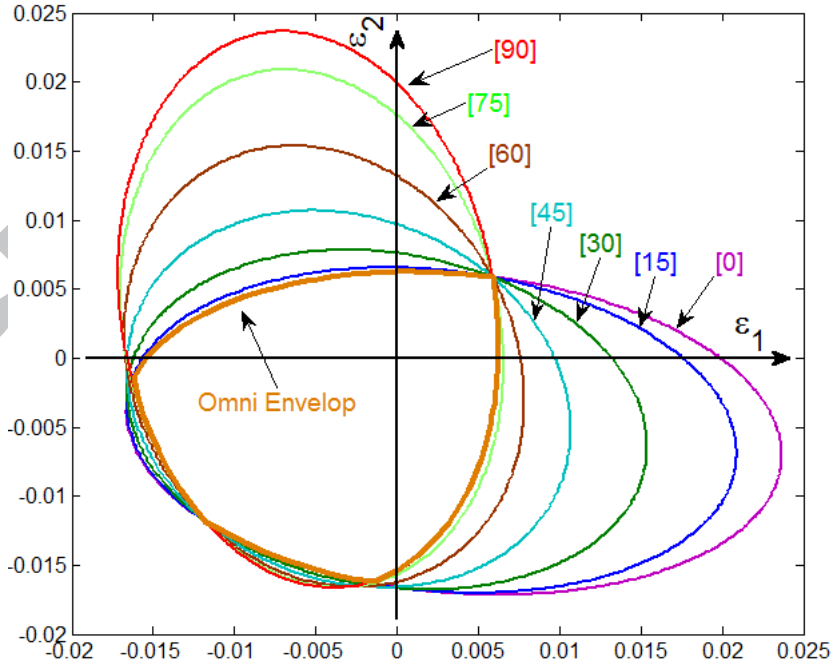

Fig. 4. Failure envelops of T800-Cytec CFRP composite in strain space

ACCEPTED MANUSCRIPT

Fig. 4 shows the failure envelops of T800/Cytec in strain space with some particular ply orientations (0°, 15°, 30°, 45°, 60°, 75°, and 90°). The properties are given in Table 2.

Table 2. Engineering constant of two CFRP composites and their strength[21]

	E_1^t	E_2	G_{12}	ν_{12}	$(\sigma_1^t)_{ult}$	$(\sigma_1^c)_{ult}$	$(\sigma_2^t)_{ult}$	$(\sigma_2^c)_{ult}$	τ_{12}^{ult}
T800/Cytec	162	9.0	5.0	0.4	3.77	1.66	0.056	0.15	0.098
T700/C-Ply 55	121	8.0	4.7	0.3	2.53	1.70	0.066	0.22	0.093

*unit: GPa

In Fig. 4, the failure envelops were determined using equal compressive/tensile moduli (λ=1). The failure envelops of different ply orientations construct a minimum shape, which was proposed as 'omni envelop' by Tsai's invariant theory[21]. It represents the first-ply-failure of a given composite for all ply orientations. Regardless of the ply orientation, the composite material is safe when the strain falls into this omni envelop.

In Table 1 and Fig. 1, it has been shown that the λ value of most of the CFRP composites is between 0.8 and 1. Fig. 5 shows the omni envelops of T800/Cytec and T700/C-Ply 55 with three λ values: 0.8, 0.9 and 1. It can be seen that, for both the two CFRP composites, the λ value has no effect on the omni envelop in the first quadrant $(\varepsilon_1 > 0, \varepsilon_2 > 0)$. For T800/Cytec, the λ value doesn't affect the omni envelop in the third quadrant $(\varepsilon_1 < 0, \varepsilon_2 < 0)$; however in the second $(\varepsilon_1 > 0, \varepsilon_2 < 0)$ and the forth $(\varepsilon_1 < 0, \varepsilon_2 > 0)$ quadrants, the omni envelop enlarges with the decrease of the λ value. It means that the CFRP composites could withstand higher strain either when $\varepsilon_1 < 0$ or $\varepsilon_2 < 0$, and the traditional failure criterion has underestimated the composite strength. The experimental results of T800/Cytec also indicated this trend in the reference [21].

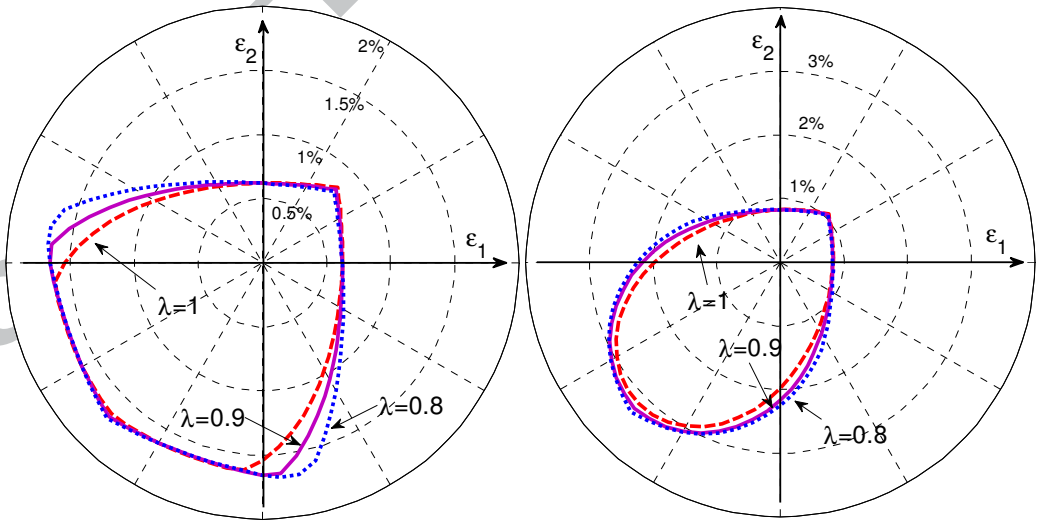

Fig. 5 Omni envelops of T800/Cytec (left) and T700/C-Ply 55 (right) with different λ values

ACCEPTED MANUSCRIPT

4. Unidirectional laminate

The terms of compressive modulus can be introduced into a modified CBT to investigate the mechanical behaviour of unidirectional laminate. Unidirectional laminate could provide both highest longitudinal modulus and strength of a given composite material. It has been widely used as the main frame of composite structures, such as wind turbine blade. In practice, the composite laminates are subjected to complicated loading rather than uniaxial force. Flexural behaviour, which includes tension, compression and shear, is normally used to evaluate the properties of composite laminates.

For a unidirectional laminate under bending, the neutral plane will have an offset to the bottom side due to the lower compressive modulus, as shown in Fig. 6.

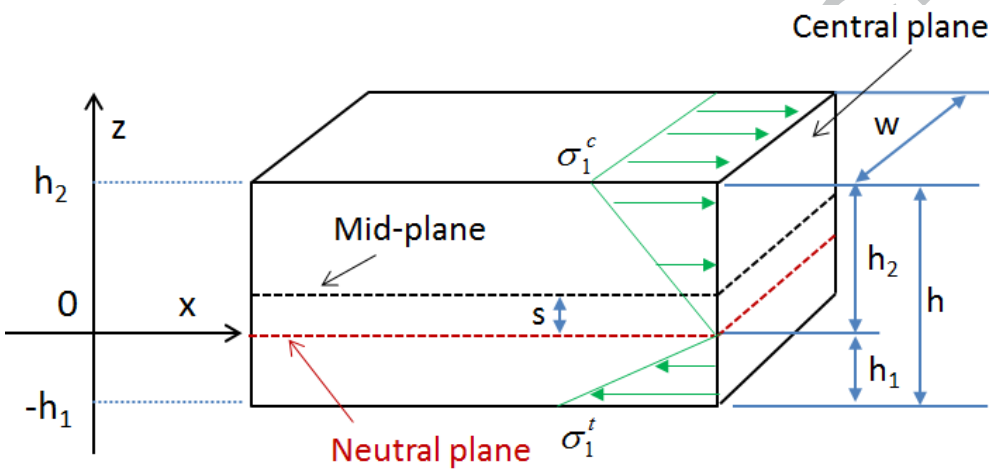

Fig. 6 Unidirectional laminate under bending. The compressive stress and tensile stress re-distribute through-thickness due to the unequal compressive and tensile moduli.

According to the principles of continuum mechanics [22], one can get the relationship between the compressive modulus, tensile modulus and apparent flexural modulus of the unidirectional laminate as described in Appendix A:

$$h_1 = \frac{h\sqrt{E_1^c}}{\sqrt{E_1^c}+\sqrt{E_1^t}} = \frac{\sqrt{\lambda}}{1+\sqrt{\lambda}}h \tag{11}$$

$$h_2 = \frac{h\sqrt{E_1^t}}{\sqrt{E_1^c}+\sqrt{E_1^t}} = \frac{1}{1+\sqrt{\lambda}}h \tag{12}$$

$$s = \frac{1-\sqrt{\lambda}}{2\left(1+\sqrt{\lambda}\right)}h \tag{13}$$

$$E^{app} = \frac{4E_1^cE_1^t}{(\sqrt{E_1^c}+\sqrt{E_1^t})^2} = \frac{4E_1^c}{\left(1+\sqrt{\lambda}\right)^2} = \frac{4\lambda E_1^t}{\left(1+\sqrt{\lambda}\right)^2} \tag{14}$$

ACCEPTED MANUSCRIPT

Equations (11-14) indicate that the apparent flexural modulus falls in between the compressive modulus and tensile modulus, and the neutral plane shifts to the side with higher stiffness. It is convenient to obtain the tensile modulus either through tensile test or calculation by rules of mixture, using fibre volume fraction, fibre tensile modulus and matrix modulus. However, the compressive modulus is much more dependent on the manufacturing process. The variation of compressive modulus may have different effects on different type of composites, which has been shown in the previous sections.

Equation (13) gives the offset (s) of the neutral plane to the mid-plane. For example, with the average λ value of CFRP composites (λ =0.9), the offset can be a quarter ply-thickness in a 16-ply unidirectional laminate or a half ply-thickness in a 32-ply laminate. The effects of unequal compressive/tensile moduli become more and more significant with the increase of laminate thickness.

If it is assume that the bending curvature through-thickness is a constant, the ratio of maximum compressive strain on the top surface to maximum tensile strain on bottom surface can be evaluated as,

$$\frac{\left(\varepsilon_1^c\right)_{\max}}{\left(\varepsilon_1^t\right)_{\max}} = \frac{h_2}{h_1} = \frac{1}{\sqrt{\lambda}} \tag{15}$$

The ratio of maximum compressive stress on the top surface to maximum tensile stress on the bottom surface is given by:

$$\frac{\left(\sigma_1^c\right)_{\max}}{\left(\sigma_1^t\right)_{\max}} = \frac{\left(\varepsilon_1^c\right)_{\max} E_1^c}{\left(\varepsilon_1^c\right)_{\max} E_1^t} = \frac{\sqrt{E_1^c}}{\sqrt{E_1^t}} = \sqrt{\lambda} \tag{16}$$

Equations (15-16) indicate that the maximum compressive strain (top surface) is higher than tensile strain (bottom surface), but the maximum tensile stress is higher than maximum compressive stress. The higher compressive strain may lead to microbuckling and compressive failure, particular in thick laminates. For example, if λ=0.8, the maximum compressive strain may be 12% higher than the maximum tensile strain. Therefore, it is more reasonable to plot the failure criteria in strain space, as has been discussed in previous section.

5. Multi-directional laminate

The terms of compressive modulus can also be introduced into a modified CLT to investigate the mechanical behaviour of multi-directional laminate. Multi-directional laminate has been used in complicated composite structures to provide variety of performance. In order to make the composite laminate self-balance, the most common multi-directional composite laminates are symmetric layup, and the middle two plies are the same ply orientations.

In the previous section, the offset of neutral plane is less than one ply-thickness. It is reasonable to make a sandwich assumption to simplify the multi-directional laminate. Consider a multi-directional laminate made of N plies (N is even number), the upper

ACCEPTED MANUSCRIPT

$(N/2-1)$ plies are treated as a compressive sheet, and the lower $(N/2-1)$ plies are treated as a tensile sheet, while the middle two plies are regarded as core material. Fig. 7 gives an illustration of this sandwich structure.

In such a sandwich structure, the compressive modulus is applied for the $(N/2-1)$ compressive plies, while the tensile modulus is applied for the $(N/2-1)$ tensile plies. Due to the symmetric geometry, the two core plies have the same ply orientations.

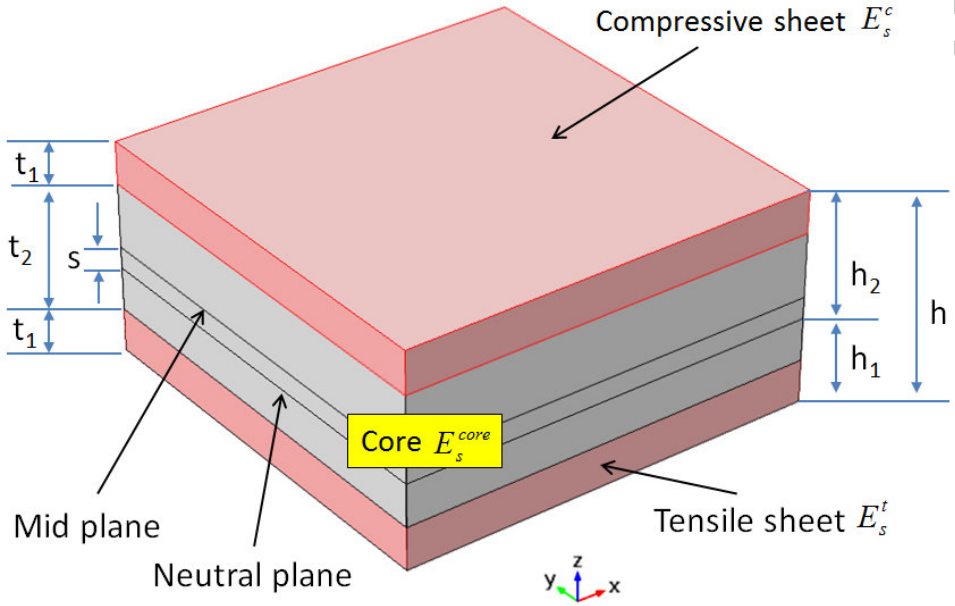

Fig. 7 Sandwich structure representation of a multi-directional laminate: compressive sheet, core, and tensile sheet. Neutral plane shifts to the bottom side but is still located in the core area.

In order to estimate the elastic modulus of the compressive and tensile sheets, their stiffness matrices should be assembled first. The deviation is shown in Appendix B. Once the ABBD matrix is assembled, inverting the matrix gives the compliance matrix:

$$[a,b;b,d]=\begin{bmatrix} a & b \\ b & d \end{bmatrix}=[A,B;B,D]^{-1} \tag{17}$$

Applying the compressive modulus into the abbd matrix of the compressive sheet, tensile modulus into the abbd matrix of tensile sheet, the apparent moduli in compressive sheet and tensile sheet can be obtained by:

$$E_s^c=\frac{12}{t_1^3 d_{11}^c}, E_s^t=\frac{12}{t_1^3 d_{11}^t} \tag{18}$$

where t_1 is the thickness of $(N/2-1)$ plies.

ACCEPTED MANUSCRIPT

Because the core only contains two plies, it has tiny effect on the total properties of the laminate. Its apparent modulus can be obtained by applying compressive modulus on the upper ply and tensile modulus on the lower ply,

$$E_s^{core} = \frac{12}{t_2^3 d_{11}^{core}} \tag{19}$$

For the purpose of comparison, the apparent flexural modulus of the whole laminate is also evaluated by CLT [23],

$$E^{app} = \frac{12}{h^3 d_{11}} \tag{20}$$

Applying the bending moment, the curvature at a given point on the composite laminate can be obtained, and then the distribution of strain through-thickness can be calculated. For example, the 3-point bending curvature at loading point is calculated as,

$$\kappa = \frac{3FL}{E^{app} w h^3} \tag{21}$$

where F is the applied flexural force, L is the span and w is the width of the laminate.

The maximum value of compressive strain and tensile strain appear on the top and bottom surfaces at the loading point:

$$\begin{aligned} \left(\varepsilon_1^c\right)_{\max} &= \frac{FLd_{11}}{4w}\left(\frac{h}{2}+s\right) \\ \left(\varepsilon_1^t\right)_{\max} &= \frac{FLd_{11}}{4w}\left(\frac{h}{2}-s\right) \end{aligned} \tag{22}$$

where the offset of neutral plane is given by:

$$s = \frac{1}{8}\frac{\left(E_s^t - E_s^c\right)\left(h^2 - t_2^2\right)}{\left(E_s^c + E_s^t\right)t_1 + E_s^{core} t_2} \tag{23}$$

In equation (22), the maximum strains in the multi-directional laminate are determined by d_{11} and s, which depend on the layup sequence and the ratio of compressive modulus to tensile modulus λ. Subsequently, the compressive stress and tensile stress of laminate are determined by the ply orientations at any particular area.

Table 3 gives the flexural properties (3-point bending) of HTS-12K/977-2 with two different λ values. The material properties are given below [4],

$$\begin{aligned} &E_1^t = 139GPa, E_2 = E_3 = 8.8GPa \\ &\nu_{12} = \nu_{13} = 0.26, \nu_{23} = 0.48 \\ &G_{12} = G_{13} = 3.0GPa, G_{23} = 4.8GPa \end{aligned}$$

ACCEPTED MANUSCRIPT

The FEA and CBT/CLT models were built based on ISO standard[24]. The laminate dimension is defined as 100 mm×15 mm×2 mm, and the span is 80 mm. The FEA solution was solved by ANSYS ACP (ANSYS Composite Prepost)[25], while the CBT and CLT models were solved by MATLAB[26]. ANSYS ACP is a pre- and post-processor integrated in ANSYS Workbench, which defines the composite layup and transfers the material properties to the main ANSYS solver.

Table 3. Normalized flexural properties of two layups of HTS-12K/977-2 when λ=0.9 and λ=1

	Multi-directional $[0/90]_{4s}$				Unidirectional $[0]_{16}$			
	FEA	CLT	FEA	CLT	FEA	CBT	FEA	CBT
	λ=0.9		λ=1		λ=0.9		λ=1	
$\varepsilon^c_{\max} : \varepsilon^t_{\max}$	1.049	1.058	0.993	1.000	1.029	1.055	0.978	1.000
E^c_s / E^t_1	—	0.661	—	0.732	—	—	—	—
E^t_s / E^t_1	—	0.732	—	0.732	—	—	—	—
d_{11}	—	0.0206	—	0.0196	—	—	—	—
$s : t$ *	—	0.23	0	0	0.47	0.21	0	0
$E^{app} : E^t_1$	1.126	1.110	1.178	1.166	0.932	0.950	0.979	1.000

*t: ply-thickness

The apparent flexural modulus evaluated by CBT/CLT and FEA were quite different between unidirectional laminate and multi-directional laminate, as shown in Table 3. This is because the top and bottom plies are longitudinal orientation in multi-directional laminate which withstand higher bending load.

For the two laminate layups (16 plies), both the FEA and CBT/CLT models give a similar trend that the maximum compressive strain represent about 5% higher than tensile strain when λ=0.9, and the neutral plane has a quarter ply-thickness offset to the bottom side. In the practical composite structures, the ply number might be far away 16 plies and these effects would be much more significant.

6. Fibre microbuckling

It has been shown in previous sections that the compressive strain is commonly higher than tensile strain when composites are subjected to bending. The higher compressive strain can increase the risk that the carbon fibres fail by microbuckling. Due to the manufacturing defects, the carbon fibres in unidirectional lamina (0°) are not perfectly aligned, typically a 2°-3° fibre misalignment as shown in Fig. 3, and the compressive failure is mostly due to fibre microbuckling [27]. Additionally, shear stress can also lead to fibre kinking and microbuckling [28].

Fig. 8 shows a schematic of a single fibre microbuckling. Because the carbon fibre is constrained by polymer within a lamina, the microbuckling is not only determined by the radius of fibre, but also the shear strength of matrix. A microbuckling term should therefore be added to the compressive strain on concave side of the fibre [29]:

ACCEPTED MANUSCRIPT

$$\varepsilon_f^c = \frac{\left(\sigma_1^c\right)_{ult}}{E_1^c} + r\frac{\pi}{\lambda_0}\gamma_m \qquad (24)$$

where $\left(\sigma_1^c\right)_{ult}$ is the compressive strength of lamina, r is the radius of carbon fibre; λ_0 is the half wavelength of microbuckling wave; γ_m is the shear strain of matrix at failure point, for many epoxy matrices, it is in the order of 5% to 7% [30].

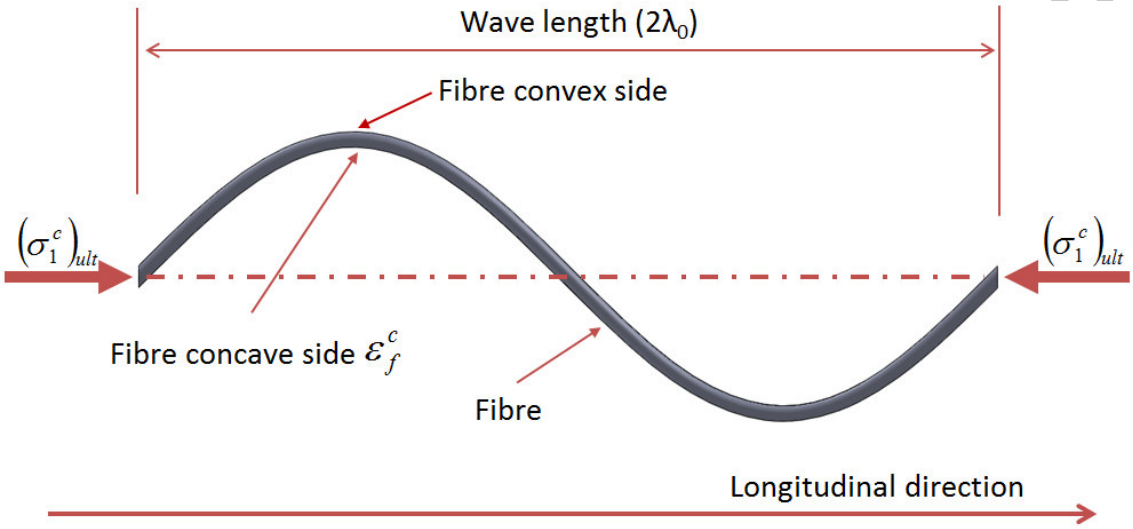

Fig. 8 A schematic of a single fibre microbuckling in unidirectional lamina. On the fibre concave side, the fibre compressive strain is expected to be higher, and the fibre is more likely to break.

In terms of statistics, the value of microbuckling half wavelength λ_0 is typically 10-15 times of fibre diameter $2r$ [5, 27, 28, 31, 32]. Substituting the compressive strength $\left(\sigma_1^c\right)_{ult} = 1.58GPa$ of HTS/977-2 and intermediate value of matrix shear failure strain ($\gamma_m = 6\%$) into equation (24), the value of maximum compressive strain on fibre concave side ε_f^c can be evaluated, as shown in Table 4.

Table 4. Value of maximum fibre compressive strain on fibre concave side ε_f^c various to the λ value and the maximum compressive strain on the top surface $\left(\varepsilon_1^c\right)_{\max}$

	λ=0.9		λ=1	
λ_0	$10\times 2r$	$15\times 2r$	$10\times 2r$	$15\times 2r$
$\left(\varepsilon_1^c\right)_{\max}$	1.26%	1.26%	1.14%	1.14%
ε_f^c	2.20%	1.89%	2.08%	1.76%

In Table 4, the fibre compressive strain ε_f^c shows a much higher value than the laminate compressive strain $\left(\varepsilon_1^c\right)_{\max}$ when the microbuckling terms is introduced, and both the laminate

ACCEPTED MANUSCRIPT

and fibre compressive strains are amplified by the λ value. In the case of λ=0.9, the maximum fibre compressive strain is about 10% higher than that of equal compressive/tensile moduli. Additionally, the half wavelength λ_0 of microbuckling also shows a significant effect on the fibre compressive strain. As a consequence, the fibres on the top surface tend to break rapidly once they are unstable.

The unequal compressive/tensile moduli have increased the risk of fibre microbuckling, which leads to a prediction that the unidirectional laminate fail by fibre microbuckling in 3-point bending test. A recent microscope image study of bending test has revealed this phenomenon [4]. Fig. 9 clearly shows the fibre kinking within a unidirectional laminate (HTS-12K/977-2). The top section of the fracture surface of unidirectional laminate was smoother inferring a fracture by shear due to microbuckling and delamination followed by the crack penetrating through the whole compressive section. Then the tensile section endured the total flexure load and finally broke rapidly by tension and fibre pull-out resulting in a rougher surface on the bottom side.

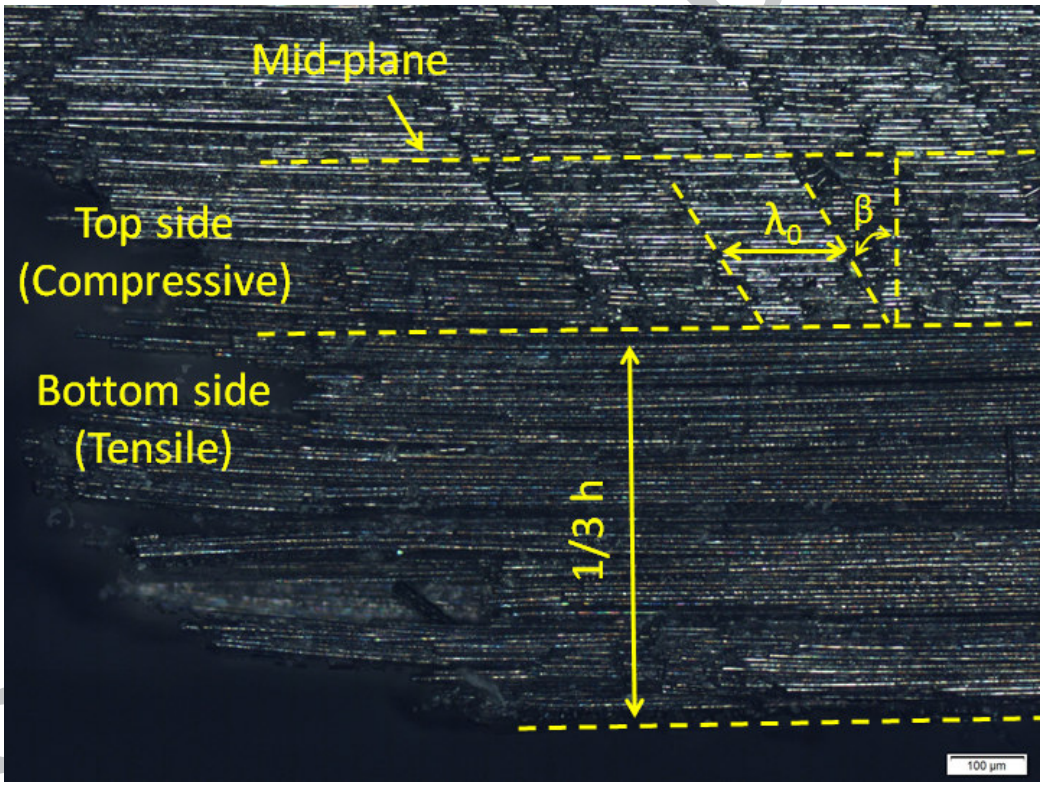

Fig. 9 Microscope image of a compressive failure of unidirectional specimen in 3-point bending. $\lambda_0 \approx 12 \times 2r$ **: half wavelength of fibre microbuckling; β=30°: orientation of microbuckling band.**

With a lower compressive modulus, the failure mode is strain dominated. As a consequence, the apparent flexural strength of the unidirectional laminate is equal to the compressive strength. In fact, the apparent flexural strength ($\left(\sigma_1^f\right)_{ult} = 1.60GPa$) evaluated by 3-point

ACCEPTED MANUSCRIPT

bending test provides the very close value to the compressive strength which was evaluated in compressive test ($\left(\sigma_1^c\right)_{ult} = 1.58GPa$)[18].

7. Conclusions

This paper, for the first time, systematically investigates the effects of unequal compressive/tensile moduli of composites. In terms of statistics, the ratios of compressive to tensile moduli of CFRP composites show an average of 0.9 with small coefficient of variation, and the compressive failure is strain dominated. The present study has successfully applied the terms of unequal compressive/tensile moduli to the failure criterion (Tsai-Wu), and predicted the failure envelops in strain space. It has been demonstrated that the λ value has no effect on the omni envelops in the first quadrant, however obvious enlargement can be found in the second and the third quadrants.

This study has proposed modified CBT and CLT methods for investigating the flexural properties of unidirectional and multi-directional laminates respectively. It has been shown that the maximum compressive strain presents about 5% higher than the maximum tensile strain when composite laminates are subjected to bending, and the neutral plane has a quarter to a half ply-thickness offset to the tensile side. These effects are more obvious in thicker laminate. Therefore, strain dominated failure criteria could generally provide more accurate prediction of composites than stress dominated failure criteria, particularly for the thicker composite laminates.

Study of unequal moduli could give a better understanding of the failure mechanisms of composites. Failure in the unidirectional laminate is initiated by the compressive strain in bending by the fibre microbuckling. The terms of unequal moduli have increased the risk of fibre microbuckling significantly. The study of microscope image has revealed the fibre kinking within a unidirectional laminate in bending.

In summary, this paper proposes that strain dominated failure criteria should be used for composites design, testing and certificate, considering the lower compressive modulus of CFRP composites.

Acknowledgements

The authors would like to thank Professor Stephen W. Tsai for his advice on omni strain transformation, Professor Long-yuan Li for his advice on FEA modelling, and the financial support of School of Marine Science and Engineering, Plymouth University.

References

1. Greene, E., *Marine composites*. 1999: Eric Greene Associates.
2. Hull, D. and T. Clyne, *An introduction to composite materials*. 1996: Cambridge university press.
3. Society, E.I., *4th Durability and Fatigue Challenges in Wind, Wave and Tidal Energy.* http://www.e-i-s.org.uk, 2014.

ACCEPTED MANUSCRIPT

4. Meng, M., et al., *3D FEA Modelling of Laminated Composites in Bending and Their Failure Mechanisms.* Composite Structures, (0).
5. Budiansky, B. and N.A. Fleck, *Compressive failure of fibre composites.* Journal of the Mechanics and Physics of Solids, 1993. **41**(1): p. 183-211.
6. Jones, R.M., *Apparent flexural modulus and strength of multimodulus materials.* Journal of Composite Materials, 1976. **10**(4): p. 342-354.
7. Jones, R.M., *Mechanics of Composite Materials with Different Moduli in Tension and Compression*. 1978, DTIC Document.
8. Naik, N. and R.S. Kumar, *Compressive strength of unidirectional composites: evaluation and comparison of prediction models.* Composite structures, 1999. **46**(3): p. 299-308.
9. De Morais, A.B., *Modelling lamina longitudinal compression strength of carbon fibre composite laminates.* Journal of composite materials, 1996. **30**(10): p. 1115-1131.
10. Chamis, C.C., *Failure Criteria for Filamentary Composites*. 1969, DTIC Document.
11. Chamis, C.C., *Design Properties of Randomly Reinforced Fiber Composites*. 1972, DTIC Document.
12. Chamis, C.C., *Analysis of the three-point-bend test for materials with unequal tension and compression properties*. 1974: National Aeronautics and Space Administration.
13. Zhou, G. and G. Davies, *Characterization of thick glass woven roving/polyester laminates: 1. Tension, compression and shear.* Composites, 1995. **26**(8): p. 579-586.
14. Zhou, G. and G. Davies, *Characterization of thick glass woven roving/polyester laminates: 2. Flexure and statistical considerations.* Composites, 1995. **26**(8): p. 587-596.
15. Mujika, F., et al., *Determination of tensile and compressive moduli by flexural tests.* Polymer testing, 2006. **25**(6): p. 766-771.
16. Carbajal, N. and F. Mujika, *Determination of compressive strength of unidirectional composites by three-point bending tests.* Polymer Testing, 2009. **28**(2): p. 150-156.
17. Jumahat, A., et al., *Fracture mechanisms and failure analysis of carbon fibre/toughened epoxy composites subjected to compressive loading.* Composite Structures, 2010. **92**(2): p. 295-305.
18. Cytec, *CYCOM 977-2 Epoxy resin system. www.cytec.com.* Technical data sheet, 2012.
19. Dept. of defense, U., *V2 Polymer matrix composites material handbook*. Composite handbook, 1997. **2**.
20. Tsai, S.W., *Theory of composites design*. 2008: Think composites Dayton.
21. Tsai, S.W. and J.D.D. Melo, *An invariant-based theory of composites.* Composites Science and Technology, 2014. **100**: p. 237-243.
22. Lai, W.M., et al., *Introduction to continuum mechanics*. 2009: Butterworth-Heinemann.
23. Gibson, R.F., *Principles of composite materials mechanics.* McGraw-Hill, 1994(ISBN O-07-023451-5).
24. ISO, I., *14125: 1998 (E).* Fibre reinforced plastic composites–determination of flexural properties, 1998.
25. ANSYS, *ANSYS reference manual.* 2013.
26. MATWORKS, *MATLAB reference manual.* 2013.
27. Soutis, C. and D. Turkmen, *Moisture and temperature effects of the compressive failure of CFRP unidirectional laminates.* Journal of Composite Materials, 1997. **31**(8): p. 832-849.
28. Liu, D., N. Fleck, and M. Sutcliffe, *Compressive strength of fibre composites with random fibre waviness.* Journal of the Mechanics and Physics of Solids, 2004. **52**(7): p. 1481-1505.
29. Berbinau, P., C. Soutis, and I. Guz, *Compressive failure of 0 unidirectional carbon-fibre-reinforced plastic (CFRP) laminates by fibre microbuckling.* Composites Science and technology, 1999. **59**(9): p. 1451-1455.

ACCEPTED MANUSCRIPT

30. Haberle, J. and F. Matthews, *A micromechanics model for compressive failure of unidirectional fibre-reinforced plastics.* Journal of composite materials, 1994. **28**(17): p. 1618-1639.
31. Soutis, C., *Compressive strength of unidirectional composites: measurement and prediction.* ASTM special technical publication, 1997. **1242**: p. 168-176.
32. Soutis, C., *Measurement of the static compressive strength of carbon-fibre/epoxy laminates.* Composites science and technology, 1991. **42**(4): p. 373-392.
33. Kaw, A.K., *Mchanics of composite materials (second edition).* Taylor & Francis Group, 2006(ISBN 0-8493-1343-0).

ACCEPTED MANUSCRIPT

ACCEPTED MANUSCRIPT

Appendix A: modified CBT

Considering an Euler beam in bending, the integration of the axial stress is zero, and the moment of normal stress (M_1) is equal to the moment (M_2) applied in the cross section:

$$\int_A \sigma_1 dA = \int_{-h_1}^{h_2} \sigma_1 w dz = w\int_{-h_1}^{0} E_1^t \varepsilon_1 dz + w\int_0^{h_2} E_1^c \varepsilon_1 dz = 0 \quad \text{(A-1)}$$

$$M_1 = \int_A \sigma_1 y dA = w\int_{-h_1}^{0} E_1^t \kappa z^2 dz + w\int_0^{h_2} E_1^c \kappa z^2 dz \quad \text{(A-2)}$$

$$M_2 = E^f I \kappa \quad \text{(A-3)}$$

If it is assumed that the specimen is long enough to neglect the out-of-plane strain, the longitudinal strain tensor is determined by:

$$\varepsilon_1 = \kappa z \quad \text{(A-4)}$$

Substituting equations (A-3) and (A-4) into equations (A-1) and (A-2),

$$E_1^t h_1^2 = E_1^c h_2^2 \quad \text{(A-5)}$$

$$E_1^t h_1^3 + E_1^c h_2^3 = \frac{E^f h^3}{4} \quad \text{(A-6)}$$

As shown in Fig. 6, the geometric relationship between h_1 and h_2 is governed by

$$h_1 + h_2 = h \quad \text{(A-7)}$$

A new parameter λ is introduced to identify the ratio of compressive modulus to tensile modulus:

$$\lambda = \frac{E_1^c}{E_1^t} \quad \text{(A-8)}$$

Combining equations (A-5), (A-6) and (A-7), one can get the relationship between compressive modulus, tensile modulus and flexural modulus of unidirectional laminate:

$$h_1 = \frac{h\sqrt{E_1^c}}{\sqrt{E_1^c} + \sqrt{E_1^t}} = \frac{\sqrt{\lambda}}{\sqrt{\lambda}+1} h \quad \text{(A-9)}$$

$$h_2 = \frac{h\sqrt{E_1^t}}{\sqrt{E_1^c} + \sqrt{E_1^t}} = \frac{1}{\sqrt{\lambda}+1} h \quad \text{(A-10)}$$

$$E^{app} = \frac{4E_1^c E_1^t}{(\sqrt{E_1^c} + \sqrt{E_1^t})^2} = \frac{4E_1^c}{\left(1+\sqrt{\lambda}\right)^2} = \frac{4\lambda E_1^t}{\left(1+\sqrt{\lambda}\right)^2} \quad \text{(A-11)}$$

ACCEPTED MANUSCRIPT

Appendix B: modified CLT

The in-plane relationship between stress and strain can be expressed by the stiffness matrix,

$$\begin{bmatrix}\sigma_1\\ \sigma_2\\ \tau_{12}\end{bmatrix}=\begin{bmatrix}Q_{11} & Q_{12} & 0\\ Q_{21} & Q_{22} & 0\\ 0 & 0 & Q_{66}\end{bmatrix}\begin{bmatrix}\varepsilon_1\\ \varepsilon_2\\ \gamma_{12}\end{bmatrix}$$

$$Q_{11}=\frac{E_1}{1-\nu_{12}\nu_{21}}, Q_{22}=\frac{E_2}{1-\nu_{12}\nu_{21}} \quad \text{(B-1)}$$

$$Q_{12}=Q_{21}=\frac{\nu_{12}E_2}{1-\nu_{12}\nu_{21}}, Q_{66}=G_{12}$$

According to Classical Laminate Theory (CLT), the extensional stiffness matrix [A], coupling matrix [B] and bending stiffness matrix [D] can be written as [33],

$$[A]=\sum_{k=1}^{N}\left(\overline{Q}_{ij}\right)_k\left(z_k-z_{k-1}\right)$$

$$[B]=\frac{1}{2}\sum_{k=1}^{N}\left(\overline{Q}_{ij}\right)_k\left(z_k^2-z_{k-1}^2\right) \quad \text{(B-2)}$$

$$[D]=\frac{1}{3}\sum_{k=1}^{N}\left(\overline{Q}_{ij}\right)_k\left(z_k^3-z_{k-1}^3\right)$$

$$\overline{Q}=T_\varepsilon^{-1}QT_\sigma$$

$$T_\varepsilon=\begin{bmatrix}c^2 & s^2 & cs\\ s^2 & c^2 & -cs\\ -2cs & 2cs & c^2-s^2\end{bmatrix} \quad \text{(B-3)}$$

$$T_\sigma=\begin{bmatrix}c^2 & s^2 & 2cs\\ s^2 & c^2 & -2cs\\ -cs & cs & c^2-s^2\end{bmatrix}$$

Assembling the [A], [B] and [D] matrices and the inverted $[a,b;b,d]$ matrix:

$$\begin{bmatrix}N_x\\ N_y\\ N_{xy}\\ M_x\\ M_y\\ M_{xy}\end{bmatrix}=\begin{bmatrix}A_{11} & A_{12} & A_{16} & B_{11} & B_{12} & B_{16}\\ A_{12} & A_{22} & A_{26} & B_{12} & B_{22} & B_{26}\\ A_{16} & A_{26} & A_{66} & B_{16} & B_{26} & B_{66}\\ B_{11} & B_{12} & B_{16} & D_{11} & D_{12} & D_{16}\\ B_{12} & B_{22} & B_{26} & D_{12} & D_{22} & D_{26}\\ B_{16} & B_{26} & B_{66} & D_{16} & D_{26} & D_{66}\end{bmatrix}\begin{bmatrix}\varepsilon_x\\ \varepsilon_y\\ \gamma_{xy}\\ \kappa_x\\ \kappa_y\\ \kappa_{xy}\end{bmatrix} \quad \text{(B-4)}$$

ACCEPTED MANUSCRIPT

$$[A,B;B,D]=\begin{bmatrix}A & B\\ B & D\end{bmatrix}$$
$$[a,b;b,d]=\begin{bmatrix}a & b\\ b & d\end{bmatrix}=[A,B;B,D]^{-1} \quad \text{(B-5)}$$

Applying the elastic properties of the compressive sheet, core and tensile sheet into equations (B-1)–(B-5), the apparent modulus in compressive sheet, core and tensile sheet can be obtained by:

$$E_s^c=\frac{12}{t_2^3 d_{11}^c}, E_s^{core}=\frac{12}{t_2^3 d_{11}^{core}}, E_s^t=\frac{12}{t_1^3 d_{11}^t} \quad \text{(B-6)}$$

The flexural modulus of the whole laminate is also evaluated by CLT [23],

$$E^{app}=\frac{12}{h^3 d_{11}} \quad \text{(B-7)}$$

For a laminate with symmetric lay-up pattern, the coupling matrix is equal to zero ($[B]=0$). Applying $M_x\neq 0, M_y=0, M_{xy}=0$ into equations (B-2)–(B-5):

$$\begin{bmatrix}\kappa_x\\ \kappa_y\\ \kappa_{xy}\end{bmatrix}=\begin{bmatrix}d_{11} & d_{12} & d_{16}\\ d_{12} & d_{22} & d_{26}\\ d_{16} & d_{26} & d_{66}\end{bmatrix}\begin{bmatrix}M_x\\ 0\\ 0\end{bmatrix} \quad \text{(B-8)}$$

$$\kappa_x=d_{11}M_x \quad \text{(B-9)}$$

In three-point bending condition, the bending moment per unit width at the loading point is evaluated as,

$$M_x=\frac{F}{2}\frac{L}{2}\frac{1}{w}=\frac{FL}{4w} \quad \text{(B-10)}$$

where F is the applied flexural force, L is the span and w is the width of the laminate.

Substituting equations (B-9) and (B-10) into equation (A-4), one can obtain the formulae for the strain and stress:

$$\varepsilon_x^z=z\kappa_x=\frac{zFLd_{11}}{4w}, \sigma_x^z=E_k\varepsilon_x^z=E_k\frac{zFLd_{11}}{4w} \quad \text{(B-11)}$$

According to equation (B-11), the longitudinal stress tensor through-thickness is not continuous. It is determined by the combination of fibre orientation, lay-up sequence, tensile modulus and compressive modulus.

On the other hand, if a pure bending moment is applied to the laminate, the integral of the longitudinal stress tensor in the cross section should be zero:

ACCEPTED MANUSCRIPT

$$\int_A \sigma_x dA = \int_{\frac{-t_2}{2}+s-t_1}^{\frac{t_2}{2}+s+t_1} \sigma_x w dz$$
$$= w\int_{\frac{-t_2}{2}+s-t_1}^{\frac{-t_2}{2}+s} E_s^t \varepsilon_x dz + w\int_{\frac{-t_2}{2}+s}^{\frac{t_2}{2}+s} E_s^{core} \varepsilon_x dz + w\int_{\frac{t_2}{2}+s}^{\frac{t_2}{2}+s+t_1} E_s^c \varepsilon_x dz = 0 \quad \text{(B-12)}$$

Integrating equation (B-12) by substituting $\varepsilon_x = \kappa_x z$,

$$s = \frac{1}{8}\frac{\left(E_s^t - E_s^c\right)\left(h^2 - t_2^2\right)}{(E_s^c + E_s^t)t_1 + E_s^{core} t_2} \quad \text{(B-13)}$$

The maximum value of stresses and strains can be evaluated as,

$$\left(\varepsilon_x^c\right)_{\max} = \frac{FLd_{11}}{4w}\left(\frac{h}{2}+s\right)$$
$$\left(\varepsilon_x^t\right)_{\max} = \frac{FLd_{11}}{4w}\left(\frac{h}{2}-s\right)$$
$$\left(\sigma_x^c\right)_{\max} = E_1^c\frac{FLd_{11}}{4w}\left(\frac{h}{2}+s\right) \quad \text{(B-14)}$$
$$\left(\sigma_x^t\right)_{\max} = E_1^t\frac{FLd_{11}}{4w}\left(\frac{h}{2}-s\right)$$

In equation (B-14), the maximum stress and strain in the multi-directional laminate are determined by d_{11} and s, which depend on the lay-up sequence and the λ value. Subsequently, the compressive stress and tensile stress of laminate are determined by the ply orientations at any particular area.

It should be noted that the subscripts (1, 2, and 3) in the above equations represent the notations in lamina level and the subscripts (x, y, and z) represent are laminate level.

Nomenclature

$[a],[b],[d]$	block matrices of $\begin{bmatrix} a & b \\ b & d \end{bmatrix}$ matrix (inversed $\begin{bmatrix} A & B \\ B & D \end{bmatrix}$ matrix)
h_1, h_2	height of tensile sheet and compressive sheet
r_1, r_2	long/short radius of ellipse
r	radius of a single fibre
s	offset of neutral plane to mid-plane
t	thickness of lamina
t_1, t_2	thickness of tensile sheet and compressive sheet

ACCEPTED MANUSCRIPT

w, h	width and height of laminate
$[A], [B], [D]$	block matrices of $\begin{bmatrix} A & B \\ B & D \end{bmatrix}$ matrix
E^{app}	apparent flexural modulus
E_1, E_2, E_3	principal elastic moduli of lamina
E_1^c, E_1^t	longitudinal compressive and tensile moduli
F_{ij}	operator of Tsai-Wu failure criterion in stress space
I	moment of inertia
M, M_x	moment
$N_{x,y,xy}, M_{x,y,xy}$	force and moment per unit length
$Q_{ij}, \overline{Q}_{ij}$	extensional compliance matrix of unidirectional and off-axis lamina
T_ε, T_σ	transformation matrices of strain and stress
U_{ij}	operator of Tsai-Wu failure criterion in strain space
V_f	fibre volume fraction
γ_m	shear strain of matrix
$\theta, \theta_1, \theta_2$	angle
κ	curvature
π	circumference ratio
λ_0	half-wavelength of fibres microbuckling
λ	ratio of compressive modulus to tensile modulus
$(\sigma_1^t)_{ult}, (\sigma_1^c)_{ult}$	ultimate longitudinal tensile and compressive strength of lamina
$(\sigma_2^t)_{ult}, (\sigma_2^c)_{ult}$	ultimate transverse tensile and compressive strength of lamina
τ_{12}^{ult}	ultimate in-plane shear strength of lamina